THE JOURNAL OF PHYSICAL CHEMISTRY Letters

Letter

pubs.acs.org/JPCL

Stability of Complex Biomolecular Structures: van der Waals, Hydrogen Bond Cooperativity, and Nuclear Quantum Effects

Mariana Rossi,*[,†,¶] Wei Fang,[‡] and Angelos Michaelides[‡]

[†]Physical and Theoretical Chemistry Lab, University of Oxford, South Parks Road, OX1 3QZ Oxford, United Kingdom

[‡]Thomas Young Centre, London Centre for Nanotechnology, and Department of Chemistry, University College London, 17-19 Gordon Street, WC1H 0AH London, United Kingdom

[¶]St. Edmund Hall, Queen's Lane, OX1 4AR Oxford, United Kingdom

Supporting Information

ABSTRACT: Biomolecules are complex systems stabilized by a delicate balance of weak interactions, making it important to assess all energetic contributions in an accurate manner. However, it is a priori unclear which contributions make more of an impact. Here, we examine stacked polyglutamine (polyQ) strands, a peptide repeat often found in amyloid aggregates. We investigate the role of hydrogen bond (HB) cooperativity, van der Waals (vdW) dispersion interactions, and quantum contributions to free energies, including anharmonicities through density functional theory and ab initio path integral simulations. Of these various factors, we find that the largest impact on structural stabilization comes from vdW interactions. HB cooperativity is the second largest contribution as the size of the stacked chain grows. Competing nuclear quantum effects make the net quantum contribution small but very sensitive to anharmonicities, vdW, and the number of HBs. Our results suggest that a reliable treatment of these systems can only be attained by considering all of these components.

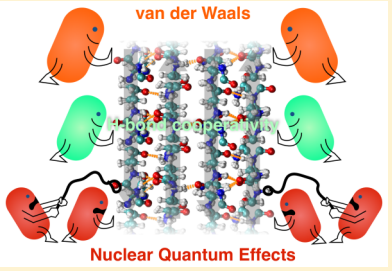

Generally, when dealing with complex systems like biomolecules, there is no easy answer as to which level of theory will be necessary to obtain a reliable structure or dynamics. The reason is that these systems are governed by a delicate balance of weak interactions, all of which can have equally large impacts on the final result. For example, taking into account the quantum nature not only of the electrons but also of the nuclei (here referred to as nuclear quantum effects, or NQE) tends to be important in systems stabilized by "weak" interactions like hydrogen bonds (HBs) and van der Waals (vdW) dispersion. NQE, in fact, can act to either stabilize or destabilize different structures.[1] The trends in stabilization and destabilization have been rationalized by the presence of competing NQE in inter- and intramolecular motions.[1,2] The effect of NQE on biological systems has been studied previously;[3,4] however, the interplay of NQE with the HB "cooperativity effect"[5−17] and vdW interactions[17] in more complex biomolecular systems with degrees of freedom spanning very different anharmonic molecular motions has not yet been quantified. In the following, we present a study that goes beyond a standard study of HB cooperativity and the role of vdW interactions and also beyond the evaluation of NQE for simple H-bonded systems.

We take as a model stacked polyglutamine (polyQ) strands, a system that is relevant also to biological processes. Genetic mutations that lead to the expansion of polyQ sequences beyond a certain length in proteins are associated with many degenerative diseases, including Huntington disease.[6,18−21] It is proposed that these polyQ tracts favor the formation of β-strands, which can then form β-hairpins and stack in aggregated H-bonded structures.[6,18] Before one can study the causes that lead to the stacking and aggregation of these structures in real peptides and biological environments, it is important to isolate and study the different qualitative contributions to their stabilization. We here simply treat an isolated, infinitely periodic, antiparallel β-sheet model system (Figure 1). Despite this simplification, the physics of the processes studied here should also be present in biological environments, even if embedded in more complex surrounding.

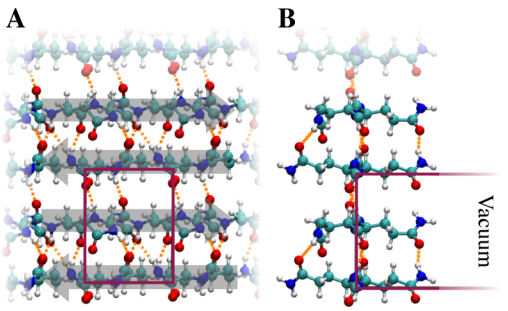

Figure 1. Schematic representation of the (a) front view and (b) side view of the periodically repeating antiparallel β-sheet polyQ structure. HBs are shown in orange. The red lines mark the unit cell. Carbon atoms are in turquoise, nitrogen atoms in blue, oxygen atoms in red, and hydrogen atoms in white.

Received: August 29, 2015
Accepted: October 5, 2015
Published: October 5, 2015

DOI: 10.1021/acs.jpclett.5b01899
J. Phys. Chem. Lett. 2015, 6, 4233−4238

The polyQ's examined here are very flexible, presenting very anharmonic potential energy surfaces. In order to estimate free energies, not only should the harmonic approximation fail, but also empirical force fields that use harmonic terms for certain energetic contributions could yield unreliable results. In addition, it is known that for an accurate description of HB cooperativity, first-principles potential energy surfaces are necessary.[10,11,17] We thus opted to perform ab initio path integral molecular dynamics (PIMD) on a density functional theory (DFT) potential energy surface to calculate dynamical and structural aspects and the quantum contributions to binding free energies of these systems. In order to evaluate the free-energy differences, we perform mass thermodynamic integrations (mass-TI)[22−25] where we take the system to its classical limit by progressively increasing its mass. Overall, we find vdW interactions and HB cooperativity to be of greater magnitude than NQE in stabilizing the stacked structures. However, we find the contributions of NQE to be extremely sensitive to the proper treatment of the two effects above and also to the inclusion or not of anharmonicities of the potential energy surface.

To begin, we fully relaxed a unit cell with two antiparallel polyQ strands using the FHI-aims program package[26] and the PBE[27]+vdW[28] functional. This structure is shown in Figure 1. For more details of these calculations, see the Supporting Information (SI). In order to calculate the buildup of cooperativity in this system, we took the geometry obtained for the infinitely periodic structure and performed single-point calculations starting from an isolated double-stranded structure, adding a new double strand at each step. These new structures are periodic only in the backbone direction and isolated in the other two, as shown pictorially in Figure 2. By not performing

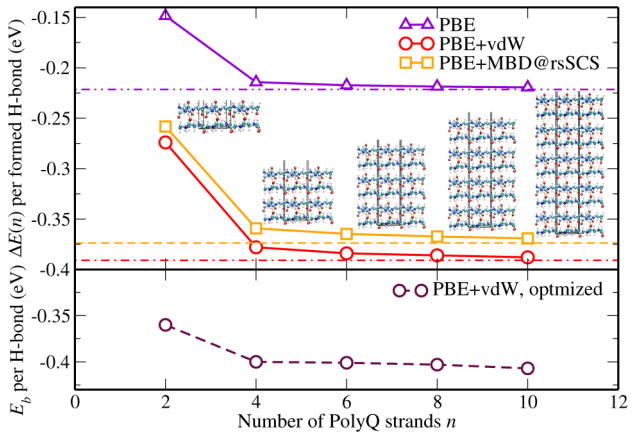

Figure 2. (Top) Energy per added antiparallel double strand ΔE_n, divided by the number of HBs formed in each step, calculated for the polyQ system. Curves are shown for the PBE[27] (purple triangles), PBE+vdW[28] (red circles), and PBE+MBD@rsSCS[29,30] (orange squares) functionals. Dotted and dashed lines represent the limit for the infinitely periodic system for the PBE, PBE+vdW, and PBE+MBD@rsSCS systems. (Bottom) Binding energy of each system with the PBE+vdW functional, with all structures fully relaxed.

further geometry optimizations, we examine the stabilization of the increasing stacked structures, approaching the infinite limit. We calculate

$$\Delta E_n = E(n) - E(n-2) - 2E_{\mathrm{opt}}(1) \tag{1}$$

where n = 2, 4, 6, 8, 10 is the number of polyQ strands considered, $E(n)$ is the total energy of the structure with n strands, and $E_{\mathrm{opt}}(1)$ is the total energy of the optimized single strand structure, here taken as our reference. In order to better visualize the buildup of the cooperativity effect, we then divided each ΔE_n by the number of new HBs formed by the addition of an antiparallel double β-strand in that step. We show in Figure 2 these quantities calculated with the PBE, PBE+vdW functional (pairwise vdW dispersion), and the PBE+MBD@rsSCS[29,30] functional, which takes into account many-body contributions to dispersion up to infinite order. We observe a 100 meV/HB energy gain in binding strength when going from 2 to 4 stacked strands and then a slow nonlinear increase of about 15 meV/HB in total until reaching the infinite limit. Adding vdW contributions is essential as it stabilizes the structures by a factor of around 1.6, without affecting much the behavior of cooperativity (consistent with what was observed for peptide helices including or not vdW dispersion[17]). A similar cooperativity behavior for parallel isolated polyQ strands has been observed in ref 8, albeit disregarding vdW contributions. Many-body dispersion energy contributions destabilize the fully periodic structure by 16 meV per HB with respect to the pairwise vdW treatment. Though not negligible, it only represents a small fraction of the full vdW contributions.

In order to assess the effect of relaxation on the structures, which is important in connection to the simulations involving dynamics presented below, we have fully relaxed all structures with the PBE+vdW functional. We evaluate a "binding" energy E_b as

$$E_b = E_{\mathrm{opt}}(n) - nE_{\mathrm{opt}}(1) \tag{2}$$

dividing this quantity by the total number of HBs at each n. This yields a curve also shown in Figure 2. As expected, the structures get stabilized with the relaxation, but the overall cooperativity trend can still be observed even if the energy drop from n = 2 to 4 is now only around 40 meV. Having established that HB cooperativity and vdW dispersion play a critical role in stabilizing polyQ structures, we turn to the role of NQE.

In order to determine the contributions of NQE to the binding free energy, we calculated the free-energy difference in going from a classical to a quantum system by performing mass-TI. To this end, we used the relation

$$\Delta F_{\mathrm{c}\to\mathrm{q}} = \int_{m_0}^{\infty} \frac{\langle K(\mu) - K_{\mathrm{class}}\rangle}{\mu}\,\mathrm{d}\mu = \int_0^1 \frac{2\langle K(m_0/g^2) - K_{\mathrm{class}}\rangle}{g}\,\mathrm{d}g \tag{3}$$

where K is the kinetic energy, m_0 is the physical mass of the atoms, μ the mass integration variable, and $g = \sqrt{m_0/\mu}$. The brackets denote an ensemble average, and the masses of all atoms are scaled in this procedure. This equation can be straightforwardly derived from the (quantum) partition function and has been proposed in many forms in a number of previous studies.[22−24] Here, we simply make use of the idea that the limit of infinite mass corresponds to the classical limit, where the quantum and the classical kinetic energy would be equal.

The quantity we are interested in calculating is the quantum contribution to the binding free energy $(\Delta F)_b$, here defined as

DOI: 10.1021/acs.jpclett.5b01899
J. Phys. Chem. Lett. 2015, 6, 4233−4238

$$(\Delta F)_b = \Delta F_{c\to q}(n) - n\Delta F_{c\to q}(1)$$
$$= \int_0^1 \frac{2}{g}[\langle K_n(m_0/g^2)\rangle - n\langle K_1(m_0/g^2)\rangle]\, dg \quad (4)$$

where $\langle K_n\rangle$ is the average kinetic energy of the system with n polyQ strands. Defined in this way, a negative $(\Delta F)_b$ means that the quantum contributions have stabilized the H-bonded system.

We perform all calculations with the i-PI[31] wrapper code connected to the FHI-aims program package and the PBE+vdW functional. PBE+vdW has been shown to provide an accurate description for a broad range of hydrogen-bonded and vdW-bonded systems (see, e.g., ref 32). Even though it is also known that generalized gradient approximations give a spurious softening of the HBs,[33,34] the computational cost of a hybrid functional would be prohibitive for the following calculations. Additional details about the calculations can be found in the SI. For comparison, we also calculated eq 4 in the harmonic approximation[25] by calculating the phonons and harmonic vibrational density of states (VDOS) of the system.

We report in Table 1 E_b as defined in eq 2, the vibrational free energies at 300 K in the harmonic approximation, and the quantum contributions to the binding free energies in the harmonic approximation and from the path integral mass integration per average total number of HBs present in the simulation. We see that in the harmonic approximation, zero-point energy, temperature, and entropic contributions amount to around 10% of E_b, from which 10% is due to quantum contributions. However, while in the harmonic approximation, NQE act to destabilize both the double- and tetra-stranded quantum structures with respect to their classical counterparts; the anharmonic effects reverse these trends and predict a total stabilization. Thus, it is only with the full path integral treatment that the expected qualitative behavior is observed.

Table 1. E_b As Defined in Equation 2, Vibrational Contribution to the "Binding" Free Energy in the Harmonic Approximation F_{vb}^{harm}, and Quantum Contributions to the Binding Free Energy in the Harmonic Approximation $(\Delta F)_b^{harm}$ and from PIMD Calculations $(\Delta F)_b$ at 300 K Per the Total Number of HBs (4 for n = 2 and 10 for n = 4)[a]

n	E_b	F_{vb}^{harm}	$(\Delta F)_b^{harm}$	$(\Delta F)_b$
2	−360	28	3	−6 ± 2
4	−400	29	3	−3 ± 1.5

[a]Energies are in meV.

The stabilization effect is very similar for the double- and tetra-stranded structures, certainly within our errors, which are reported in Table 1. Also, even though the quantum contribution is small, we are here comparing quite different structures (isolated and H-bonded polyQ strands). Because for the H-bonded structures the total contributions are of the order of k_BT at room temperature (see Figure S2 of the SI) and in a more realistic situation there should be competing conformers within this energy window, these effects may actually play an important role.

In order to understand the origins of the observed NQE contributions, we plot the integrands of eq 4 in the harmonic approximation and from the path integral mass-TI, both shown in Figure 3a. The shapes are qualitatively similar, even if there is no a priori reason for them to exhibit the exact same shape, but anharmonic effects substantially pull the curves to lower energies. This suggests greater softening of the vibrational modes in the anharmonic case with respect to the harmonic one. Similar effects have been seen for low-energy modes in other peptides including anharmonicities for classical nuclei.[35,36]

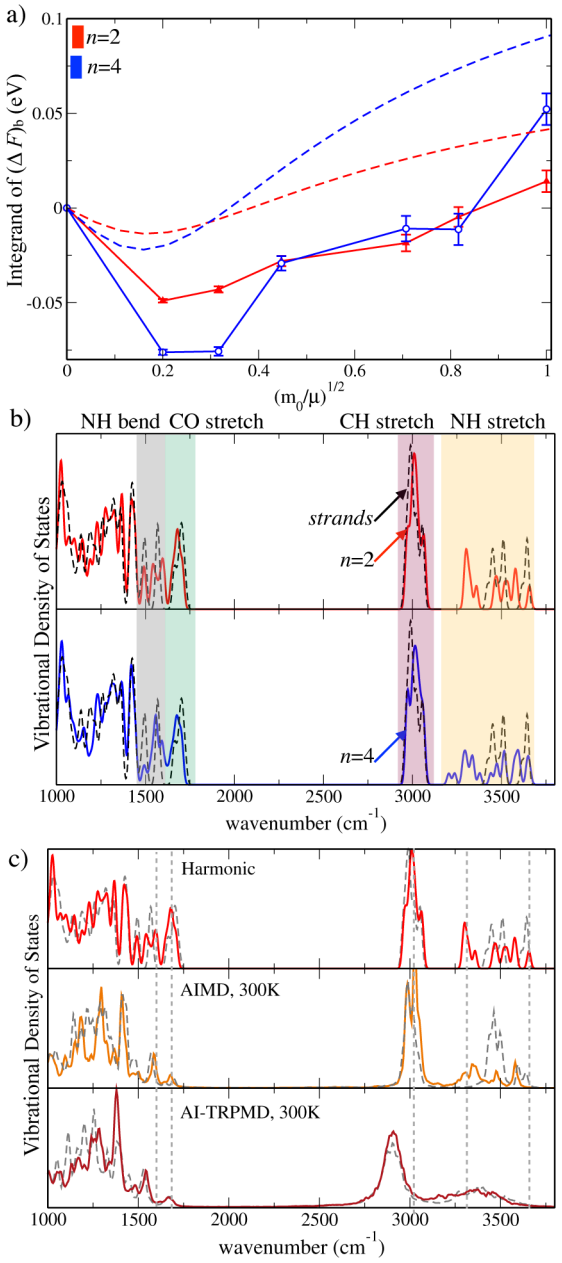

Figure 3. (a) Integrand of eq 4 in the harmonic approximation (dashed lines) and fully anharmonic (PIMD) case (full lines) for n = 2 and 4, on a PBE+vdW potential energy surface. (b) PBE+vdW harmonic VDOS for the single polyQ strands (black dashed line), for the n = 2 structure (red, upper pannel), and for the n = 4 structure (blue, lower panel). (c) PBE+vdW VDOS in the harmonic approximation (upper panel), from the Fourier transform of the velocity autocorrelation function with classical nuclei at 300 K (middle panel), and with quantum nuclei using the TRPMD method at 300 K (lower panel) for n = 2 and the respective single strands (shown as dashed lines). The simulations were run for 10 ps.

In Figure 3b, we show the changes in the VDOS that we observe upon forming HBs, in the harmonic approximation.

DOI: 10.1021/acs.jpclett.5b01899
J. Phys. Chem. Lett. 2015, 6, 4233−4238

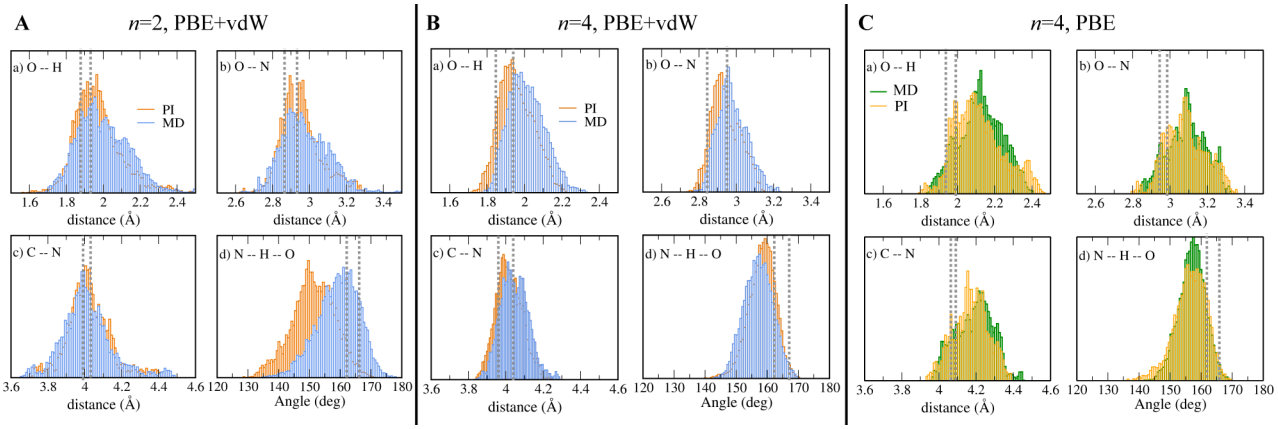

Figure 4. Structural quantities for the classical AIMD simulations and the PIMD ones, for (A) $n = 2$ with the PBE+vdW functional, (B) $n = 4$ with the PBE+vdW functional, and (C) $n = 4$ with the PBE functional. We consider only backbone HBs and report O···H bond lengths, the O···N bond lengths, the C···N bond lengths (rough measure of the backbone distance), and the HB angles formed by N···H···O atoms. The dotted lines in each plot correspond to the values for $n = 2$ and the interval of values for $n = 4$ for that distance or angle found in the respective fully relaxed structure.

Especially in the region between 3200 and 3400 cm^{-1}, we observe a softening of the H-bonded NH stretches as n increases, which is consistent with the strengthening of the HBs with chain length observed due to cooperativity. In the NH bending region, it is hard to pinpoint differences because the spectra are very congested. It can be shown (see SI, Figure S5) that the shape of the integrand in Figure 3a, at least in the harmonic approximation, does not come only from competing contributions (softening and hardening) from vibrational modes directly connected to the HBs but from an intricate interplay involving destabilizing contributions from backbone vibrations, CH stretches, and NH bendings and stabilizing contributions from CO and NH stretches. In Figure 3c, we focus on the structure with two antiparallel polyQ strands and calculate as well the VDOS given by the Fourier transform of the velocity autocorrelation function from an ab initio MD (AIMD) run (i.e., with classical nuclei) and from the newly proposed thermostated ring polymer molecular dynamics (TRPMD) method,[37] at 300 K. TRPMD is equivalent to PIMD for static properties but in addition can also give an approximation to time correlation functions. Comparing the AIMD case at 300 K with the harmonic one (0 K), we observe a softening of the high-frequency NH stretches, but most of the rest of the spectrum remains the same. With TRPMD, there is a much more pronounced softening of both NH and CH stretches by as much as 100 cm^{-1}. Because TRPMD produces typically broader peaks in the spectra,[37,38] it is hard to analyze exactly which modes are more softened upon HB formation in the quantum case (compare solid and dashed lines). However, the larger softening observed in the TRPMD VDOS can explain the pronounced dips in the integrand reported in Figure 3a and the fact that the structures are stabilized by the quantum contributions in the fully anharmonic case. We stress that this effect would not be captured by classical anharmonicity alone.

Structural aspects can also give important physical insight. We performed PIMD and classical ab initio *NVT* MD simulations with the PBE and PBE+vdW functionals for the double- and tetra-stranded structures for 10 ps, at 300 K. We considered only backbone HBs and compared O···H bond lengths, O···N bond lengths, C···N bond lengths (rough measure of the backbone distance), and HB angles. These quantities are shown in Figure 4A for $n = 2$, in Figure 4B for $n = 4$ with the PBE+vdW functional, and in Figure 4C for $n = 4$ with the PBE functional. For $n = 2$, the softening of the NH bendings is clearly reflected in the shift of the distribution of HB angles to lower values in the quantum case. It is hard to observe any other very pronounced effect except perhaps for a small shift to shorter O···H distances in the quantum case. Compared to Figure 3c middle and lower panels (AIMD and AI-TRPMD), this means that we would either need much more sampling to observe an effect here or the backbone HBs (connected to the NH stretches) are not that much softened in the quantum case. When going to $n = 4$ with the PBE+vdW functional, the effects are more pronounced. All distances are shifted to smaller values in the quantum case, even if just barely for the backbone. The differences in angles between the classical and quantum cases is small, but now, the angles are stiffer in the quantum case (this stiffening trend of the angles is consistent with ref 1 for stronger HBs). This points to a considerable hardening due to NQE of the NH bendings in the tetra-stranded structure, which is again consistent with the competing NQE picture and could explain why we do not see a much larger energetic stabilization for the $n = 4$ case than for the $n = 2$ case. It is possible that for even larger structures, the stabilization brought about by the softening of the NH stretches wins over. It is interesting to note in Figure 4C that when analyzing the dynamics of $n = 4$ with the PBE functional, both the distances between atoms and the angle distributions are essentially on top of one another even if the distances show considerably larger mean values than those in the PBE+vdW case. This is to be expected because these HBs are weaker than the PBE+vdW ones.

In passing, we mention that we also performed mass-TI simulations, changing only the masses of the hydrogen atoms in the system to reach that of deuterium for the isolated strands and for $n = 2$. We found that the deuterated structure is ever so slightly destabilized but only by 1 meV per HB. Within our error bars, this value is not significant but perhaps worth reporting.

We have reported a systematic study on the combination of so-called "weak" interactions that contribute to structure stabilization of model antiparallel stacked polyQ (a peptide repeat often found in amyloid diseases), namely, HB cooperativity, vdW dispersion interactions, and NQE including dynamics and a fully anharmonic potential energy surface. We have drawn a complex picture of the interplay of these effects in

DOI: 10.1021/acs.jpclett.5b01899
J. Phys. Chem. Lett. 2015, 6, 4233−4238

larger biomolecular systems that had not been previously quantified.

We find that among these interactions, vdW dispersion represents the largest contribution to HB stabilization, followed by HB cooperativity as the chain grows. The impact of NQE, though small (a few meV per HB), is seen to depend on its interplay with cooperativity, vdW, and whether one takes into account the full anharmonicity of the potential energy surface or not. Anharmonic effects change the sign of the NQE contributions to the free energy with respect to the harmonic estimate, most likely due to the observed overall softening of the vibrational modes caused by the inclusion of NQE on dynamics. We thus find that in an anharmonic picture, NQEs represent a small stabilization component in these structures. The strengthening of the HBs by vdW and cooperativity also enhances the competing nature of NQEs. Structural properties are visibly affected by NQE differently depending on the size of the chain and the addition of vdW, but for the energy contributions that we calculated, we did not observe a strong impact, as long as one goes beyond the harmonic approximation. These effects may be important for structures that are in close energetic competition, for example, slightly different folding motifs.

The system studied here is just a first step in order to understand these structures from a quantum mechanical perspective. With growing computational capacity, it would be ideal to employ better electronic structure methods (NQE on structural properties can be affected by the choice of potential) and consider systems closer to the biological reality. Nevertheless, the results presented here suggest that for a reliable prediction of stability of close-competing conformational motifs in larger polypeptides, which can be decisive in studying folding and misfolding of proteins, a high-level (quantum) treatment of nuclei, electronic structure, and anharmonicities is necessary. This, of course, also underlines the need to train empirical potentials on high-level potential energy surfaces.

■ ASSOCIATED CONTENT

Supporting Information

The Supporting Information is available free of charge on the ACS Publications website at DOI: 10.1021/acs.jpclett.5b01899.

Technical details of the simulations and convergence tests (PDF)

Geometry parameters (ZIP)

■ AUTHOR INFORMATION

Corresponding Author

*E-mail: mariana.rossi@chem.ox.ac.uk.

Notes

The authors declare no competing financial interest.

■ ACKNOWLEDGMENTS

The authors thank Michele Ceriotti and David Manolopoulos for relevant discussions and input in the paper. M.R. acknowledges funding from the German Research Foundation (DFG) under Project RO 4637/1-1. A.M. is supported by the European Research Council under the European Union's Seventh Framework Programme (FP/2007-2013)/ERC Grant Agreement Number 616121 (HeteroIce project) and the Royal Society through a Royal Society Wolfson Research Merit Award. We are grateful to the UKCP consortium (EP/F036884/1) for access to ARCHER.

■ REFERENCES

(1) Li, X.-Z.; Walker, B.; Michaelides, A. Quantum Nature of the Hydrogen Bond. *Proc. Natl. Acad. Sci. U. S. A.* **2011**, *108*, 6369−6373.

(2) Habershon, S.; Markland, T. E.; Manolopoulos, D. E. Competing Quantum Effects in the Dynamics of a Flexible Water Model. *J. Chem. Phys.* **2009**, *131*, 024501.

(3) Perez, A.; Tuckerman, M. E.; Hjalmarson, H. P.; von Lilienfeld, O. A. Enol Tautomers of Watson-Crick Base Pair Models Are Metastable Because of Nuclear Quantum Effects. *J. Am. Chem. Soc.* **2010**, *132*, 11510−11515.

(4) Wang, L.; Fried, S. D.; Boxer, S. G.; Markland, T. E. Quantum Delocalization of Protons in the Hydrogen-bond Network of an Enzyme Active Site. *Proc. Natl. Acad. Sci. U. S. A.* **2014**, *111*, 18454−18459.

(5) Cruzan, J.; Braly, L.; Liu, K.; Brown, M.; Loeser, J.; Saykally, R. Quantifying Hydrogen Bond Cooperativity in Water: VRT Spectroscopy of the Water Tetramer. *Science* **1996**, *271*, 59−62.

(6) Buchanan, L. E.; Carr, J. K.; Fluitt, A. M.; Hoganson, A. J.; Moran, S. D.; de Pablo, J. J.; Skinner, J. L.; Zanni, M. T. Structural Motif of Polyglutamine Amyloid Fibrils Discerned with Mixed-isotope Infrared Spectroscopy. *Proc. Natl. Acad. Sci. U. S. A.* **2014**, *111*, 5796−5801.

(7) Santra, B.; Michaelides, A.; Scheffler, M. On the Accuracy of Density-Functional Theory Exchange-Correlation Functionals for H Bonds in Small Water Clusters: Benchmarks Approaching the Complete Basis Set Limit. *J. Chem. Phys.* **2007**, *127*, 184104.

(8) Rossetti, G.; Magistrato, A.; Pastore, A.; Carloni, P. Hydrogen Bonding Cooperativity in PolyQ β-Sheets from First Principle Calculations. *J. Chem. Theory Comput.* **2010**, *6*, 1777−1782.

(9) Tsemekhman, K.; Goldschmidt, L.; Eisenberg, D.; Baker, D. Cooperative Hydrogen Bonding in Amyloid Formation. *Protein Sci.* **2007**, *16*, 761−764.

(10) Salvador, P.; Kobko, N.; Wieczorek, R.; Dannenberg, J. J. Calculation of trans-Hydrogen-Bond 13C-15N Three-Bond and Other Scalar J-Couplings in Cooperative Peptide Models. A Density Functional Theory Study. *J. Am. Chem. Soc.* **2004**, *126*, 14190−14197.

(11) Ireta, J.; Neugebauer, J.; Scheffler, M.; Rojo, A.; Galván, M. Density Functional Theory Study of the Cooperativity of Hydrogen Bonds in Finite and Infinite α-Helices. *J. Phys. Chem. B* **2003**, *107*, 1432−1437.

(12) Van Duijnen, P. T.; Thole, B. T. Cooperative Effects in α-helices: An Ab Initio Molecular-Orbital Study. *Biopolymers* **1982**, *21*, 1749−1761.

(13) Elrod, M.; Saykally, R. Many-Body Effecs in Intermolecular Forces. *Chem. Rev.* **1994**, *94*, 1975−1997.

(14) Xantheas, S. Cooperativity and Hydrogen Bonding Network in Water Clusters. *Chem. Phys.* **2000**, *258*, 225−231.

(15) Suhai, S. Cooperativity and Electron Correlation Effects on Hydrogen Bonding in Infinite Systems. *Int. J. Quantum Chem.* **1994**, *52*, 395−412.

(16) Dannenberg, J. J. Cooperativity in Hydrogen Bonded Aggregates. Models for Crystals and Peptides. *J. Mol. Struct.* **2002**, *615*, 219−226.

(17) Tkatchenko, A.; Rossi, M.; Blum, V.; Ireta, J.; Scheffler, M. Unraveling the Stability of Polypeptide Helices: Critical Role of van der Waals Interactions. *Phys. Rev. Lett.* **2011**, *106*, 118102.

(18) Kar, K.; Hoop, C. L.; Drombosky, K. W.; Baker, M. A.; Kodali, R.; Arduini, I.; van der Wel, P. C.; Horne, W. S.; Wetzel, R. β-Hairpin-Mediated Nucleation of Polyglutamine Amyloid Formation. *J. Mol. Biol.* **2013**, *425*, 1183−1197.

(19) Roethlein, C.; Miettinen, M.; Borwankar, T.; Buerger, J.; Mielke, T.; Kumke, M. U.; Ignatova, Z. Architecture of Polyglutamine-Containing Fibrils from Time Resolved Fluorescence Decay. *J. Biol. Chem.* **2014**, *289*, 26817.

DOI: 10.1021/acs.jpclett.5b01899
J. Phys. Chem. Lett. 2015, 6, 4233−4238

(20) Landrum, E.; Wetzel, R. Biophysical Underpinnings of the Repeat Length Dependence of Polyglutamine Amyloid Formation. *J. Biol. Chem.* **2014**, *289*, 10254−10260.
(21) Hoop, C. L.; Lin, H.-K.; Kar, K.; Hou, Z.; Poirier, M. A.; Wetzel, R.; van der Wel, P. C. A. Polyglutamine Amyloid Core Boundaries and Flanking Domain Dynamics in Huntingtin Fragment Fibrils Determined by Solid-State Nuclear Magnetic Resonance. *Biochemistry* **2014**, *53*, 6653−6666.
(22) Ceriotti, M.; Markland, T. E. Efficient Methods and Practical Guidelines for Simulating Isotope Effects. *J. Chem. Phys.* **2013**, *138*, 014112.
(23) Marsalek, O.; Chen, P.-Y.; Dupuis, R.; Benoit, M.; Méheut, M.; Bacic, Z.; Tuckerman, M. E. Efficient Calculation of Free Energy Differences Associated with Isotopic Substitution Using Path-Integral Molecular Dynamics. *J. Chem. Theory Comput.* **2014**, *10*, 1440−1453.
(24) Pérez, A.; von Lilienfeld, O. A. Path Integral Computation of Quantum Free Energy Differences Due to Alchemical Transformations Involving Mass and Potential. *J. Chem. Theory Comput.* **2011**, *7*, 2358−2369.
(25) Habershon, S.; Manolopoulos, D. E. Thermodynamic Integration from Classical to Quantum Mechanics. *J. Chem. Phys.* **2011**, *135*, 224111.
(26) Blum, V.; Gehrke, R.; Hanke, F.; Havu, P.; Havu, V.; Ren, X.; Reuter, K.; Scheffler, M. Ab Initio Molecular Simulations With Numeric Atom-Centered Orbitals. *Comput. Phys. Commun.* **2009**, *180*, 2175−2196.
(27) Perdew, J.; Burke, K.; Ernzerhof, M. Generalized Gradient Approximation Made Simple. *Phys. Rev. Lett.* **1996**, *77*, 3865−3868.
(28) Tkatchenko, A.; Scheffler, M. Accurate Molecular Van Der Waals Interactions from Ground-State Electron Density and Free-Atom Reference Data. *Phys. Rev. Lett.* **2009**, *102*, 073005.
(29) Ambrosetti, A.; Reilly, A. M.; DiStasio, R. A.; Tkatchenko, A. Long-range Correlation Energy Calculated from Coupled Atomic Response Functions. *J. Chem. Phys.* **2014**, *140*, 18A508.
(30) Tkatchenko, A.; DiStasio, R. A.; Car, R.; Scheffler, M. Accurate and Efficient Method for Many-Body van der Waals Interactions. *Phys. Rev. Lett.* **2012**, *108*, 236402.
(31) Ceriotti, M.; More, J.; Manolopoulos, D. E. i-PI: A Python Interface for Ab Initio Path Integral Molecular Dynamics Simulations. *Comput. Phys. Commun.* **2014**, *185*, 1019−1026.
(32) Klimeš, J.; Michaelides, A. Perspective: Advances and Challenges in Treating van der Waals Dispersion Forces in Density Functional Theory. *J. Chem. Phys.* **2012**, *137*, 120901.
(33) Wang, L.; Ceriotti, M.; Markland, T. E. Quantum Fluctuations and Isotope Effects in Ab Initio Descriptions of Water. *J. Chem. Phys.* **2014**, *141*, 104502.
(34) Santra, B.; Michaelides, A.; Scheffler, M. Coupled Cluster Benchmarks of Water Monomers and Dimers Extracted from Density-functional Theory Liquid Water: The Importance of Monomer Deformations. *J. Chem. Phys.* **2009**, *131*, 124509.
(35) Rossi, M. *Ab Initio Study of Alanine-based Polypeptide Secondary-structure Motifs in the Gas Phase*. Ph.D. thesis, Technical University Berlin and Fritz Haber Institute, 2011; http://opus.kobv.de/tuberlin/volltexte/2012/3429/.
(36) Rossi, M.; Scheffler, M.; Blum, V. Impact of Vibrational Entropy on the Stability of Unsolvated Peptide Helices with Increasing Length. *J. Phys. Chem. B* **2013**, *117*, 5574−5584.
(37) Rossi, M.; Ceriotti, M.; Manolopoulos, D. E. How to Remove the Spurious Resonances from Ring Polymer Molecular Dynamics. *J. Chem. Phys.* **2014**, *140*, 234116.
(38) Rossi, M.; Liu, H.; Paesani, F.; Bowman, J.; Ceriotti, M. Communication: On the Consistency of Approximate Quantum Dynamics Simulation Methods for Vibrational Spectra in the Condensed Phase. *J. Chem. Phys.* **2014**, *141*, 181101.

DOI: 10.1021/acs.jpclett.5b01899
J. Phys. Chem. Lett. 2015, 6, 4233−4238